r3
Reference: *Biol. Bull.* **165**: 791–810. (December, 1983)

MARINE BIOLUMINESCENCE SPECTRA MEASURED WITH AN OPTICAL MULTICHANNEL DETECTION SYSTEM

EDITH A. WIDDER, MICHAEL I. LATZ, AND JAMES F. CASE

Department of Biological Sciences and the Marine Sciences Institute, University of California, Santa Barbara, California 93106

Abstract

The emission spectra of 70 bioluminescent marine species were measured with a computer controlled optical multichannel analyzer (OMA). A 350 nm spectral window is simultaneously measured using a linear array of 700 silicon photodiodes, coupled by fiber optics to a microchannel plate image intensifier on which a polychromator generated spectrum is focused. Collection optics include a quartz fiber optic bundle which allows spectra to be measured from single photophores. Since corrections are not required for temporal variations in emissions, it was possible to acquire spectra of transient luminescent events that would be difficult or impossible to record with conventional techniques. Use of this system at sea on freshly trawled material and in the laboratory has permitted acquisition of a large collection of bioluminescence spectra of precision rarely obtained previously with such material. Among unusual spectral features revealed were organisms capable of emitting more than one color, including: *Umbellula magniflora* and *Stachyptilum superbum* (Pennatulacea), *Parazoanthus lucificum* (Zoantharia), and *Cleidopus gloria-maris* (Pisces). Evidence is presented that the narrow bandwidth of the emission spectrum for *Argyropelecus affinis* (Pisces) is due to filters in the photophores.

Introduction

Measurements of bioluminescence spectra, especially from fragile marine organisms, are complicated by the frequently dim and transient nature of their luminescence. Recently developed intensified optical multichannel detectors, capable of simultaneous measurement of an entire spectral region, are well suited to overcoming these difficulties. Here we describe the use of one such optical multichannel analyzer (OMA) system sufficiently robust for use at sea as well as in the laboratory, and present the first collection of bioluminescence spectra acquired with it. This system is adaptable to the extreme range of variables encountered in taking spectra of living systems, namely potentially broad spectral range, wide range of possible luminous intensities, erratic time-intensity characteristics of light emission, and the variable size and structure of the light emitting tissues.

Materials and Methods

Theory of operation

The detector (Table I and Fig. 1) is an intensified silicon photodiode (ISPD) linear array placed in the image plane of a polychromator. Light focused on the entrance

Received 12 August 1983; accepted 21 September 1983.

Abbreviations: FWHM, full width at half maximum; ISPD, intensified silicon photodiode; NBS, National Bureau of Standards; OMA, optical multichannel analyzer; S.D., standard deviation; S/N, signal to noise ratio; UV, ultraviolet; λ_{max}, wavelength at peak emission.

slit of the polychromator is dispersed by the diffraction grating across the 700 intensified detector elements (25 μm $\times$ 2.5 mm each) of the ISPD linear array. Photons striking the reverse-biased diodes create electron-hole pairs in the semiconductor material which discharge the equivalent capacitance of the diode. When the array is scanned, the amount of recharging required by each diode (pixel) is a measure of the number of electron-hole pairs formed. Since pixel position can be directly related to the wavelength of incident photons, the charge per pixel represents a spectrum of the light focused on the entrance slit.

Light may be directly integrated on the detector for periods ranging from 16 ms to more than 20 s. Since the entire spectral window under examination is measured simultaneously rather than sequentially, as in the conventional spectrophotometer, there is no need to correct for time dependent changes in the emission, which are common in bioluminescence. The limit of integration is determined by the dark current which is kept low by thermoelectric cooling of the detector. Computer control (Digital Equipment Corporation LSI-11) of integration time provides the sensitivity and dynamic range necessary for dealing with the wide range of luminous intensities encountered in bioluminescent organisms.

Collection optics

Because the size and structure of light emitting sources varied widely in the organisms studied, considerable flexibility was required of the polychromator collection optics. Initially, we used the convenient method of positioning the organism in front

TABLE I

Instrumentation

Detector	EG&G-PARC Model 1420 intensified silicon photodiode (ISPD) linear array, composed of 1024 diodes (each 25 μm $\times$ 2.5 mm). The microchannel plate intensifier is fiber optically coupled to 700 of the detector elements.
Detector controller	EG&G-PARC Model 1218.
Computer console	EG&G-PARC Model 1215 and Model 1217 outboard disc drive. Allows storage and manipulation of up to 60 spectra per diskette.
Plotter	Hewlett-Packard 7045B X-Y recorder.
Polychromator	ISA Model HR-320, 0.32 m Czerny-Turner f/4.8 with a 58 $\times$ 58 mm 152 grooves/mm grating blazed at 250 nm. Reciprocal linear dispersion, 0.49 nm/diode.
Collection optics	Two all-quartz systems, aperture matched to the polychromator and used to focus the image of the source onto the entrance slit. Large aperture system: a 50 mm objective lens fixed at 100 mm from the 75 mm field lens. Fiber optic system: a Welch Allyn circle to line converter, 50 cm ultraviolet light pipe, with a 2mm bundle diameter terminating in a linear output 7 mm $\times$ 0.9 mm, focused with a 10 mm cylindrical lens.
Calibration system	Oriel Model 6047 low pressure mercury spectral lamp.
	Optronics Model 245H 45 watt quartz tungsten-halogen standard of total and spectral irradiance.
	Optronics Model 65 precision current source.
	Optronics Model UV-40 40 watt deuterium arc standard of spectral irradiance.
	Optronics Model 45 deuterium lamp precision current source.

of the entrance slit without input optics (Seliger *et al.*, 1964; Swift *et al.*, 1977). Since this procedure may degrade the resultant spectrum by scattering unfocused, stray light in the polychromator, two interchangeable quartz lens systems were developed to focus the luminescent source at the polychromator entrance slit. For large luminescent sources we used a 50 mm objective lens and a 75 mm field lens mounted in a fixed tube, baffled and aperture-matched to the polychromator (Fig. 1A). The input port for the tube was 1.76 cm in diameter and designed so that a luminescent source positioned in the input plane produced a focused image at the entrance slit of the polychromator. For smaller luminescent sources such as photophores (*ca.* 1 mm diameter) or other discrete luminescent regions of organisms, we used a 2 mm diameter quartz fiber optic terminated in a 7 mm × 0.9 mm rectangular output focused on the slit by a 10 mm focal length fused silica cylindrical condenser lens. This system was also baffled and aperture matched to the polychromator (Fig. 1B).

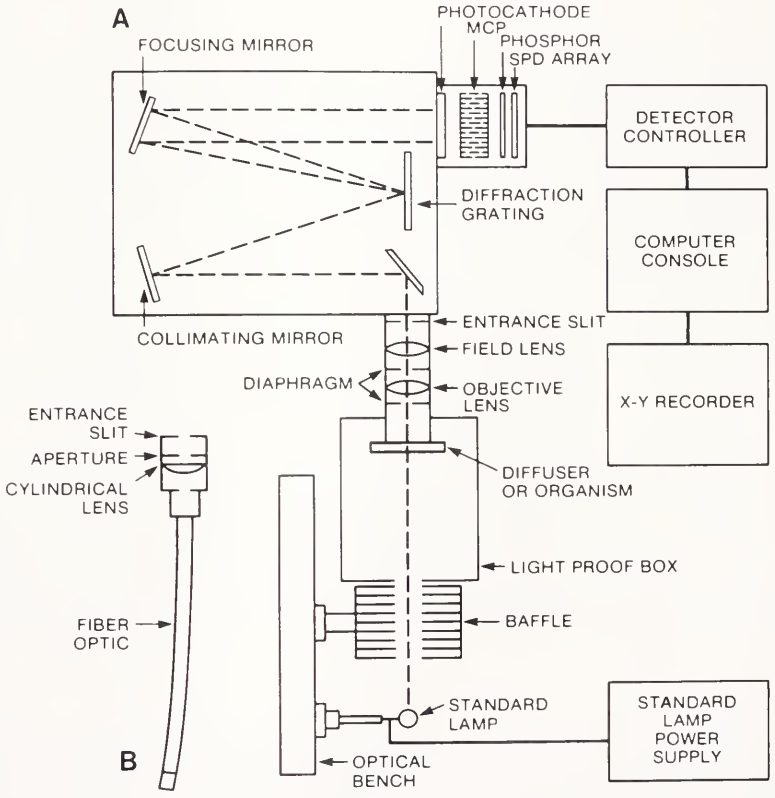

FIGURE 1. Schematic of apparatus for measuring emission spectra in calibration configuration. (A) Bioluminescence or standard lamp output is focused by the input optics on the entrance slit of the polychromator. The spectrum from the diffraction grating falls on the cathode of the detector, where it is intensified and then detected by a linear array of silicon photodiodes. The detector is operated through the detector controller under computer control. Spectral distributions are stored on floppy disk, analyzed, and then plotted on an X-Y recorder. The system is calibrated by tungsten-halogen and deuterium standard lamps and a mercury spectral lamp. The output from these calibration sources is collimated by a series of baffles and diffused by a quartz ground disc before entering the input optics to the polychromator. (B) Alternate collection optics consist of a 2 mm diameter quartz fiber optic light pipe terminating in a linear output, focused on the entrance slit by a cylindrical lens. Not drawn to scale.

Sensitivity

The combination of the microchannel plate intensifier with the long integration times attainable with the silicon photodiode array allow attainment of high sensitivity. The minimum detectable signal (signal to noise ratio = 2) for an ISPD at the normal operating temperature of 0°C is 4 photons/s/diode with an integration time of 10 s (Talmi, 1982). Insertion of the f/4.8 polychromator and collection optics between the ISPD and the source resulted in a minimum detectable signal at the input of the fiber optic of 7,150 photons/s at 475 nm with a 1 mm slit and 20 s integration time. With the double lens system, which had an input area 81 times that of the fiber optic, 45,000 photons/s at 475 nm were required.

This level of sensitivity permitted measurement of the spectrum of one flash of a single dinoflagellate, *Pyrocystis fusiformis,* and, using integration times of 10 to 20 s, it was possible to measure the spectrum of any source visible to the dark-adapted human eye.

Calibration

Since the input optics and spectral window were changed frequently while working at sea, a method of field calibration was necessary. A low-pressure mercury spectral lamp (Table I) was used for wavelength calibration. A spectral irradiance standard and precision current source (Table I) were used to correct for nonuniformities in channel-to-channel sensitivity and for detector and polychromator efficiencies. The calibration function was generated as the ratio of the measured spectrum to the true spectrum (Fig. 2A), which was determined from the NBS referenced calibration data supplied with the lamp. To be accurate, the calibration function must be generated under the same conditions as the spectrum to which it will be applied. To do this the unfocused standard lamp beam was collimated, and then diffused by a quartz ground glass of known transmission. This diffuser served as the radiant source to the polychromator and was positioned at the input of the optical system at what would be the plane of focus of the bioluminescent organism or tissue.

Stray light, often a problem in single stage polychromators, is a fraction of a percent of the total irradiance (Talmi, 1982) and is insignificant at the low intensities characteristic of bioluminescence. However, the intense red emission of the tungsten-halogen standard lamp produced stray light that was a significant percentage of the lamp's much weaker emissions below 400 nm. To insure accuracy of the correction curve in the near UV, we used an NBS referenced deuterium arc lamp to generate the correction function below 400 nm.

Data analysis

Spectra were stored on floppy disks, with automatic subtraction of the dark charge, background spectrum. Postexperiment manipulation of data primarily involved division of the emission spectrum by the correction curve stored in memory and digital smoothing of the data using a Savitzky-Golay least-square polynomial algorithm (Savitzky and Golay, 1964; Edwards and Willson, 1974) (Fig. 2B). The running least squares fit was to a second degree polynomial over a 25 channel smoothing range. This smoothing range was well below the recommended value of 70% of the narrowest spectral feature observed (Edwards and Willson, 1974) and, therefore, facilitated identification of such spectral features as λ_{max} and FWHM without decreasing resolution. The smoothing function was applied from 1 to 10 times depending on the signal to noise ratio (S/N) of the spectrum. The signal to noise ratio of each spectrum was

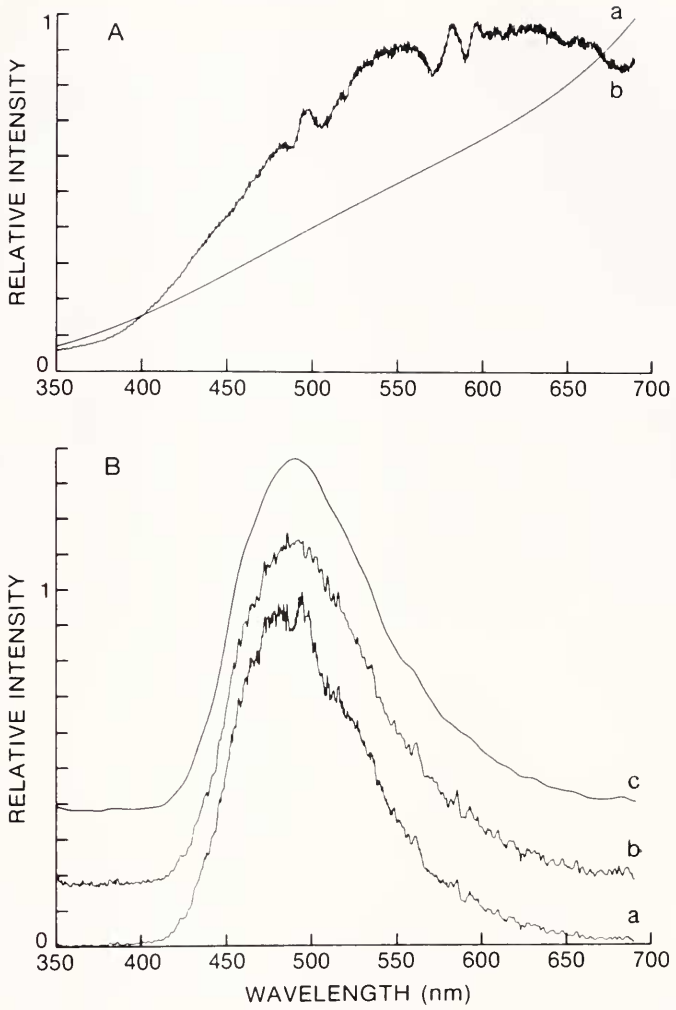

FIGURE 2. (A) Real *versus* ideal curves for spectral output of the tungsten-halogen standard lamp. Derived from 100 scans, each 16.6 ms in duration, using the double lens collection optics with 0.025 mm entrance slit. Relative intensity is shown as a function of wavelength. (a) Ideal curve calculated from a third degree polynomial curve fit to the data supplied with the lamp. (b) Standard lamp spectral output as measured with OMA. Fluctuations in the measured spectrum are the result of non-uniformities in the sensitivity of the system. A correction curve is generated by dividing curve (b) by curve (a). (B) Effects of data correction and analysis on emission from a colony of the tunicate, *Pyrosoma atlanticum*, using double lens optics and 1 mm slit. (a) Uncorrected spectrum. Apparent bimodality is explained by fluctuation in the real standard lamp curve (A-b), with the result that the corrected spectrum (b) is unimodal. The corrected spectrum which has been smoothed five times (c) has a λ_{max} = 491 nm, FWHM = 96, and S/N = 99. Each curve is shown on a similar relative scale but is displaced vertically for clarity.

computed as the ratio of the signal at λ_{max} to the root mean square noise over the whole spectral range (calculated by first subtracting the smoothed from the unsmoothed corrected spectrum). Other computer operations included calibration of channel number to wavelength value and generation of the ideal standard lamp curve using a third degree polynomial curve fit to the data supplied with the lamps.

Accuracy and resolution

Since bioluminescent emissions occur over the entire visible spectrum, it is desirable to examine as broad a spectral range as possible when examining new organisms. Consequently we have used a 152 grooves/mm plane grating which provides a spectral coverage of about 350 nm and a spectral bandwidth of 0.5 nm/diode. Geometric registration on the ISPD is excellent, ±1 diode (Talmi and Simpson, 1980); therefore, wavelength accuracy was ±0.5 nm with the 152 grooves/mm grating. Resolution was a function of the grating and the slit width and was empirically determined as the product of the reciprocal linear dispersion and the FWHM of one of the mercury lines (Felkel and Pardue, 1979). Experimentally determined resolution was: 2 nm using the 0.025 mm slit, 3 nm with the 0.1 mm slit, and with the 1 mm slit it was 9 nm using the fiber optic input and 20 nm using the lens system or no collection optics. Resolution and accuracy were also a function of the relative brightness of the source. In order to examine this effect, a C^{14} activated phosphor disc (λ_{max} 524 nm) was attached to the input of the double lens system and five readings were taken with the 1 mm slit at each of several different integration times. At integration times producing signal to noise ratios of 150 and above, the average standard deviation was less than 1.5 nm for λ_{max} and less than 0.8 nm for FWHM measurements. With signal to noise ratios between 30 and 150, the average S.D. was 6.5 nm for λ_{max} and 0.9 nm for FWHM. At S/N ratios below 30, the S.D. of λ_{max} and FWHM measurements were 19 and 10 nm respectively. Examples of spectra with S/N ratios within these three different ranges are shown in Figure 3A. For signal to noise ratios above 150 the smoothing function was applied only once, for ratios between 30 and 150 it was applied a maximum of 5 times, and below 30 it was applied a maximum of 10 times (Fig. 3B).

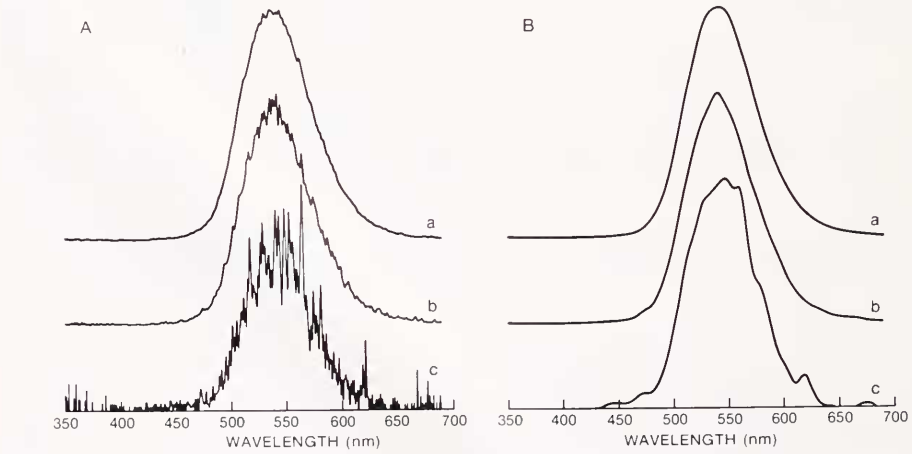

FIGURE 3. Determination of accuracy as a function of source intensity using a constant output C^{14} activated phosphor. Using the double lens optics with 1 mm slit, different integration times yielded spectra with different signal to noise ratios. (A) Corrected spectra with (a) S/N = 229, (b) S/N = 71, and (c) S/N = 11. With the lowest signal to noise ratio (c), noise spikes are pronounced. (B) Smoothed spectra from (A). The curve with S/N = 229 (a) was smoothed once, λ_{max} = 524 nm, FWHM = 74 nm. (b) Curve with S/N = 71 underwent five smoothings, λ_{max} = 524 nm, FWHM = 73 nm. (c) Curve with lowest signal to noise ratio (S/N = 11) was smoothed 10 times, λ_{max} = 530 nm, FWHM = 75 nm. Note noise bumps. All six curves are plotted on a relative linear intensity scale.

Collection and handling of organisms

Deep-living organisms were collected from the Catalina, East Cortez, San Clemente, Santa Barbara, and Velero Basins off the coast of Southern California during 1982 and 1983. Benthic samples were taken with a 5 ft beam trawl and a near-bottom beam trawl with a 2 × 10 ft mouth opening; midwater collections were made with an opening-closing midwater Tucker trawl (10 × 10 ft opening) fitted with an opaque, thermally-insulated cod-end. The pelagic holothurian *Scotoanassa* was collected by the deep submersible "Alvin." Sorted animals were placed in chilled sea water (4–8°C) and maintained in light-proof coolers until use. All measurements were made within 4 h after collection. Coastal and subtidal animals were collected locally in the Santa Barbara Basin, near Santa Barbara, or near Scripps Institution of Oceanography, La Jolla, California, by trawling or SCUBA diving and maintained in the laboratory in aquaria with flow-through, sand-filtered sea water (18°C). A few specimens were obtained from laboratory cultures or a commercial aquarium. Specimens were placed for testing in quartz glassware containing sea water or held in air and positioned in front of the detector collection optics. In some cases, bioluminescence was stimulated or enhanced by 1×10^{-3} *M* norepinephrine, 1×10^{-4} g/ml serotonin, or 2% hydrogen peroxide. Otherwise, unstimulated or mechanically stimulated emissions were measured. Specimens were preserved in 5 or 10% buffered formalin for subsequent identification. Reference specimens have been deposited in the Invertebrate Zoology Collection, Santa Barbara Museum of Natural History.

Results

Spectral data

Table II lists 70 bioluminescent species from which we have obtained spectra using the OMA. They are arranged taxonomically and the spectral features listed are the wavelength at peak emission (λ_{max}) and the width at half the maximum value (FWHM). The signal to noise ratio (S/N) is included as a measure of relative accuracy. Whenever a given organism was available on more than one occasion, spectra were taken. Multiple spectra were averaged and the mean with standard deviation was determined. Spectra were grouped for averaging in three S/N ranges: above 150, between 150 and 30, and below 30. Readings below 30 were not listed if better measurements were available. Measurements made at different slit widths were kept separate, and in cases where different collection optics had a significant effect on the values, they were listed separately. This was most apparent when the fiber bundle collection optics were used with the 1 mm slit. The greater resolution of the fiber bundle at this slit width was due to its 0.9 mm linear output width and was most apparent for spectra with narrow bandwidths.

Over the year during which these spectra were collected an effort was made to insure accurate calibration and correction factors. One obvious independent check of the entire system is the reproducibility of the spectral data and comparison of our measurements with accurately known bioluminescence spectra from other laboratories. *Renilla* has an extremely stable emission spectrum (Wampler *et al.,* 1973) and as a result it has been suggested that it might serve as an "emission standard . . . for routine calibration checks" (Wampler, 1978). Following this advice, we measured specimens of the local species, *Renilla köllikeri,* many times throughout the year with different collection optics, slit widths, and polychromator settings (Table II). The values measured remained in good agreement and also compared well with measurements made in other laboratories (Reynolds, 1978; Wampler *et al.,* 1973).

TABLE II

Species	λ_{max}* (nm) $\bar{X} \pm$ S.D. (n)	FWHM (nm)	S/N	Slit (mm)	Remarks
Phylum Bacteria					
Photobacterium leiognathi	481	79	373	1.0[b]	
	481	77	24	0.05[c]	
Photobacterium phosphoreum	483	75	385	1.0[b]	
	481	73	241	0.025[b]	
	481	73	43	0.025[c]	
Vibrio fischeri	492 ± 1 (2)	94 ± 0	294 ± 18	1.0[b]	
	493	95	132	0.1[b]	
	496	94	71	0.025[b]	
Vibrio fischeri Y-1	540	81	333	1.0[b]	20°C
	495	101	72	1.0[b]	29°C
Vibrio harveyi	488	96	246	1.0[b]	
	483	93	96	0.025[c]	
Isolates from *Abyssicola macrochir* (Pisces: Macrouridae)	486	73	103	1.0[b]	
Isolates from *Coelorhynchus japonicus* (Pisces: Macrouridae)	481	77	34	1.0[b]	
Phylum Dinophyta					
Pyrocystis fusiformis	471	35	154	1.0[a]	
	472 ± 0 (2)	32 ± 3	152 ± 7	0.1[a,b]	
Pyrocystis lunula	472	38	125	1.0[a]	
	472 ± 0 (2)	34 ± 0	136 ± 2	0.1[a,b]	

Pyrocystis noctiluca	472	35	180	1.0[a]	
	472	33	170	0.1[b]	
Gonyaulax polyedra	474	35	53	1.0[a]	
	472	30	71	0.1[b]	
Phylum Cnidaria					
Maresearsia praeclara	473	64	42	1.0[c]	
Periphylla periphylla	463 ± 1 (3)	76 ± 4	57 ± 40	1.0[a,c]	
Atolla wyvillei	462 ± 1 (3)	79 ± 4	88 ± 48	1.0[a,c]	
Renilla köllikeri	509	22	199	1.0[a]	
	509	25	130	1.0[a]	
	509	23	97	1.0[a]	rachis
	509	25	47	1.0[a]	polyps
	509 ± 1 (3)	30 ± 0	276 ± 111	1.0[b,c]	
	509 ± 2 (5)	30 ± 2	100 ± 27	1.0[b,c]	
	508 ± 1 (5)	22 ± 1	113 ± 35	0.1[a,b]	
	508	21	123	0.025[a]	
Distichoptilum verrilli	508 ± 1 (5)	31 ± 11	141 ± 38	1.0[a]	
Stylatula elongata	511 ± 1 (4)	25 ± 1	84 ± 27	1.0[a]	
Acanthoptilum annulatum	510 ± 1 (3)	26 ± 1	77 ± 31	1.0[a]	
Acanthoptilum album	510 ± 1 (2)	25 ± 0	162 ± 27	1.0[a]	
Stachyptilum superbum	503 ± 2 (2)	29 ± 3	196 ± 21	1.0[a]	
	505 ± 0 (2)	43 ± 4	71 ± 56	1.0[b]	
	533	44	251	1.0[a]	
	533	58	78	1.0[b]	
Umbellula magniflora	501	30	56	1.0[a]	bottom of stalk
	500	46	81	1.0[b]	bottom of stalk
	499 ± 2 (2)	71 ± 25	15 ± 18	1.0[a]	middle of stalk
	470	62	44	1.0[a]	top of stalk
	489 ± 3 (2)	70 ± 2	8 ± 4	1.0[a]	polyps
	498	101	14	1.0[b]	polyps

TABLE II (*Continued*)

Species	λ_{max}* (nm) $\bar{X} \pm$ S.D. (n)	FWHM (nm)	S/N	Slit (mm)	Remarks
Pennatula phosphorea var. *californica*	500	53	45	1.0[a]	
Parazoanthus lucificum	500	121	154	1.0[b]	
	502	108	145	1.0[a]	same colony
	574	94	56	1.0[a]	
Epizoanthus cf. induratum	500	93	67	1.0[c]	
Phylum Ctenophora					
Mnemiopsis sp.	480	83	47	1.0[b]	from St. Augustine, Florida
Beroë cf. cucumis	484	83	45	1.0[c]	
	483	83	23	1.0[c]	
Beroë cf. forstali	482	86	89	1.0[a]	
Beroë sp.	484 ± 2 (6)	80 ± 7	83 ± 29	1.0[c]	
	484	77	21	1.0[a]	
Phylum Arthropoda					
Vargula hilgendorfii	465	82	165	1.0[c]	dried
	465	83	101	1.0[b]	dried
	465 ± 8 (3)	84 ± 5	70 ± 8	0.1[a,b,c]	dried
	469 ± 4 (2)	85 ± 1	76 ± 8	0.05[c]	dried
Vargula tsujii	466 ± 0 (2)	87 ± 1	118 ± 40	1.0[c]	dried
Gaussia princeps	489	77	186	1.0[c]	secretion
	486 ± 3 (8)	75 ± 3	50 ± 18	1.0[a,c]	secretion
	483	75	31	0.1[c]	secretion
	488	74	34	0.05[c]	secretion
Gnathophausia ingens	484 ± 3 (11)	83 ± 2	61 ± 32	1.0[a,b,c]	secretion

Scina cf. *rattrayi*	439	70	48	1.0[a]	antennae[1]
Euphausia pacifica	470 ± 2 (3)	46 ± 4	92 ± 26	1.0[c]	
Nyctiphanes simplex	467	44	64	1.0[b]	
Nematoscelis difficilis	483	81	43	1.0[b]	
Hymenodora sp.	456	70	67	1.0[a]	secretion
Parapasiphea sulcatifrons	454	64	13	1.0[c]	
Sergestes similis	472 ± 4 (2)	58 ± 6	12 ± 9	1.0[a]	cephalothorax[1]
	472	63	10	1.0[a]	post. light organ[1]
Sergia phorcus	472	97	4	1.0[c]	mid-body photophores
Phylum Mollusca					
Abraliopsis falco	[421] 466	105	12	1.0[c]	subocular photophores[2]
Cranchia scabra	[480 ± 1] 510 ± 2 (2)	78 ± 2	47 ± 3	1.0[a]	medial subocular photophores[1]
	[483] 511	77	63	1.0[a]	lateral subocular photophores[1]
	[481] 511	83	24	1.0[a]	subocular photophores
Galiteuthis phyllura	[472] 506	59	16	1.0[a]	subocular photophores[1]
Helicocranchia pfefferi	[476 ± 3] 502 ± 0 (2)	92 ± 0	9 ± 1	1.0[a]	
Vampyroteuthis infernalis	466 ± 3 (2)	75 ± 1	21 ± 8	1.0[a,c]	finbase photophore *in situ*
	461	75	136	1.0[a]	finbase photophore *in situ*[1]
	461 ± 3 (7)	74 ± 1	70 ± 35	1.0[a,c]	excised finbase photophore
	464	79	156	1.0[a]	excised finbase photophore[1]
	464	77	44	1.0[a]	excised finbase photophore[1]
Phylum Echinodermata					
Scotoplanes globosa	463 ± 1 (2)	71 ± 3	33 ± 2	1.0[a]	
Scotoanassa hollisi	463 ± 0 (2)	75 ± 3	59 ± 21	1.0[c]	

TABLE II (*Continued*)

Species	λ_{max}* (nm) $\bar{X} \pm$ S.D. (n)	FWHM (nm)	S/N	Slit (mm)	Remarks
Pannychia moselyii	465	70	7	1.0[a]	
Ophiopholis cf. longispina	[483 ± 1] 511 ± 1 [545 ± 0] (2)	98 ± 6	46 ± 6	1.0[a]	
Phylum Chordata					
Subphylum Tunicata					
Oikopleura dioica	483	95	45	1.0[c]	
Pyrosoma atlanticum	488 ± 1 (2)	93 ± 4	34 ± 2	1.0[a]	
	492 ± 1 (2)	98 ± 2	75 ± 35	1.0[b]	pigmented colonies
Pyrosomella cf. verticillata	491 ± 6 (3)	95 ± 2	89 ± 5	1.0[c]	
	483	96	33	0.1[c]	
Subphylum Vertebrata					
Eurypharynx pelecanoides	472	76	13	1.0[a]	dorsal epidermis
Argyropelecus affinis	482 ± 6 (3)	31 ± 8	83 ± 40	1.0[a,c]	
	486	29	15	1.0[a]	post. photophores
	484	53	9	1.0[a]	ant. photophores; tips excised
Borostomias panamensis	484	68	51	1.0[c]	post-orbital photophore
Aristostomias scintillans	481	59	99	1.0[c]	post-orbital photophore[3]
Chauliodus macouni	478	85	11	1.0[a]	
Stomias atriventer	479 ± 1 (3)	75 ± 1	104 ± 26	1.0[c]	dermis; tail region
	476	77	75	1.0[c]	dermis; dorsal mid-body region
	481	71	47	1.0[c]	upper jaw
	483	79	26	1.0[c]	ant. photophores
Stomias sp.	478	77	68	1.0[a]	dermis; ventral caudal fin[3]
	470	85	20	1.0[a]	ant. photphore[3]
	497	69	45	1.0[a]	photophores[3]

Idiacanthus antrostomus	472	82	38	1.0[c]	posterior photophores
	471 ± 2 (2)	77 ± 1	18 ± 1	1.0[c]	ant. photophores
Triphoturus mexicanus	469 ± 2 (6)	62 ± 1	90 ± 55	1.0[a,c]	infracaudal organ
	469	61	158	1.0[a]	supracaudal organ
	469 ± 3 (3)	60 ± 2	105 ± 25	1.0[c]	caudal organs
	461	91	6	1.0[c]	photophores
Lampanyctus ritteri	469 ± 0 (2)	62 ± 2	86 ± 52	1.0[c]	infracaudal organ
Stenobrachius leucopsarus	474	62	204	1.0[a]	infracaudal organ
	475 ± 3 (3)	62 ± 3	94 ± 34	1.0[a]	infracaudal organ
	473 ± 1 (2)	64 ± 1	71 ± 31	1.0[c]	caudal organs
Lampadena urophaos	468 ± 1 (2)	62 ± 0	63 ± 9	1.0[c]	caudal organs
Porichthys notatus	489 ± 2 507 ± 3 (4)	73 ± 3	78 ± 52	1.0[a,b]	ventral photophores[3]
	484 501	75	69	1.0[a]	1 ventral photophore[3]
	485 507	73	25	1.0[a]	1 ventral photophore[3]
	486 504	67	12	1.0[a]	1 supraorbital photophore[3]
	491 511	69	13	1.0[a]	2 suborbital photophores[3]
Porichthys myriaster	491 ± 0 512 ± 2 (2)	76 ± 0	59 ± 18	1.0[a]	ventral photophores[3]
Oneirodes acanthias	480	74	108	1.0[c]	esca
Oneirodes sp.	477	80	190	1.0[a]	esca
Cleidopus gloria-maris	506	92	264	1.0[a]	ant. region left organ; adult
	506	85	200	1.0[a]	mid-region left organ; adult
	510	88	317	1.0[a]	mid-region right organ; adult
	503	86	304	1.0[a]	post. region left organ; adult
	555	120	199	1.0[a]	ant. region right organ; juvenile
	523	120	219	1.0[a]	mid-region right organ; juvenile
	522	122	232	1.0[a]	mid-region left organ; juvenile
	516	101	217	1.0[a]	post. region right organ; juvenile
Anomalops katoptron	493	94	53	1.0[a]	suborbital photophore

[a] Fiber bundle collection optics.
[b] Double lens collection optics.
[c] No collection optics.
[1] Bioluminescence stimulated or enhanced by hydrogen peroxide.
[2] Bioluminescence enhanced by serotonin.
[3] Bioluminescence stimulated or enhanced by norepinephrine.
* Secondary peaks in brackets.

Spectral range

In general, spectra were confined to the range of 400 nm to 700 nm. Occasionally spectra extended into the near UV. The greatest emission noted below 400 nm was by the squid *Abraliopsis falco* (Fig. 4E). Minor emission below 400 nm was also seen in the crustaceans *Scina* and *Sergestes* (Figs. 4A and 4C). The range of spectral maxima measured extended from 439 nm for *Scina* to 574 nm for *Parazoanthus* (Table II).

Spectral shapes

Examples of the observed variety in spectral shapes are shown in Figure 4. Most spectra were structureless and unimodal (Fig. 4A), with bandwidths ranging between 26 nm (*Argyropelecus affinis*, Fig. 4A) and 100 nm (*Pyrosoma atlanticum*, Fig. 2B) with an average of 75 to 80 nm. The emission spectrum for *Argyropelecus* was notable for its unusually narrow bandwidth. Among the other organisms measured, the narrowest bandwidths among the structureless unimodal emissions were those from the caudal organs of the myctophids (*Triphoturus mexicanus, Lampanyctus ritteri, Stenobrachius leucopsarus,* and *Lampadena urophaos*) (Table II). Emission spectra for these fish exhibited bandwidths of about 62 nm.

It is known that the photophores of *Argyropelecus* consist of deeply placed tissue that transmits light to the ventral surface through light-pipe-like structures which contain pigmented filters (Denton *et al.*, 1970). To determine if the filters in the ventral photophores are responsible for the unusual narrowness of the emission spectrum, a 1 mm strip was cut from the anterior photophores of one specimen. The emission spectrum from this region was measured with the fiber bundle collection optics and compared with a spectrum taken from the posterior uncut region of the same specimen. Removal of the ventral anterior strip increased the bandwidth more than 20 nm over the spectrum measured from the posterior intact photophores (Fig. 5).

Essentially unimodal spectra were observed with some structural complexity, commonly seen as a long wavelength shoulder as in all the pennatulids and dinoflagellates measured (Fig. 4B) and less commonly with a short wavelength shoulder as seen in *Sergestes, Parazoanthus* and the Y-1 strain of *Vibrio fischeri* (Fig. 4C).

Porichthys exhibited the only emission spectrum with bimodal peaks of approximately equal intensity (Fig. 4D). All squids measured had bimodal emission spectra with short wavelength secondary peaks and long wavelength shoulders (Fig. 4E). The only trimodal spectrum measured was that of the brittle star *Ophiopholis* which had both short and long wavelength secondary peaks (Fig. 4F).

Spectral variation within species

In several instances different emission spectra were observed from different colonies of the same species. The most notable example of this was the pennatulid, *Stachyptilum superbum* (Table II). One 60 min beam trawl at 600 m in the Santa Barbara Basin yielded hundreds of these sea pens. Visual inspection revealed that approximately 1 out of every 100 colonies had a much yellower emission than the majority. Measurements of the emission spectra demonstrated a 30 nm difference in emission maxima and a slightly broader bandwidth for the yellow emitters. No morphological differences were found to distinguish the two variants.

Another example of this phenomenon was seen in a colony of *Parazoanthus lucificum*. The emission spectrum for the colony as initially measured with the double

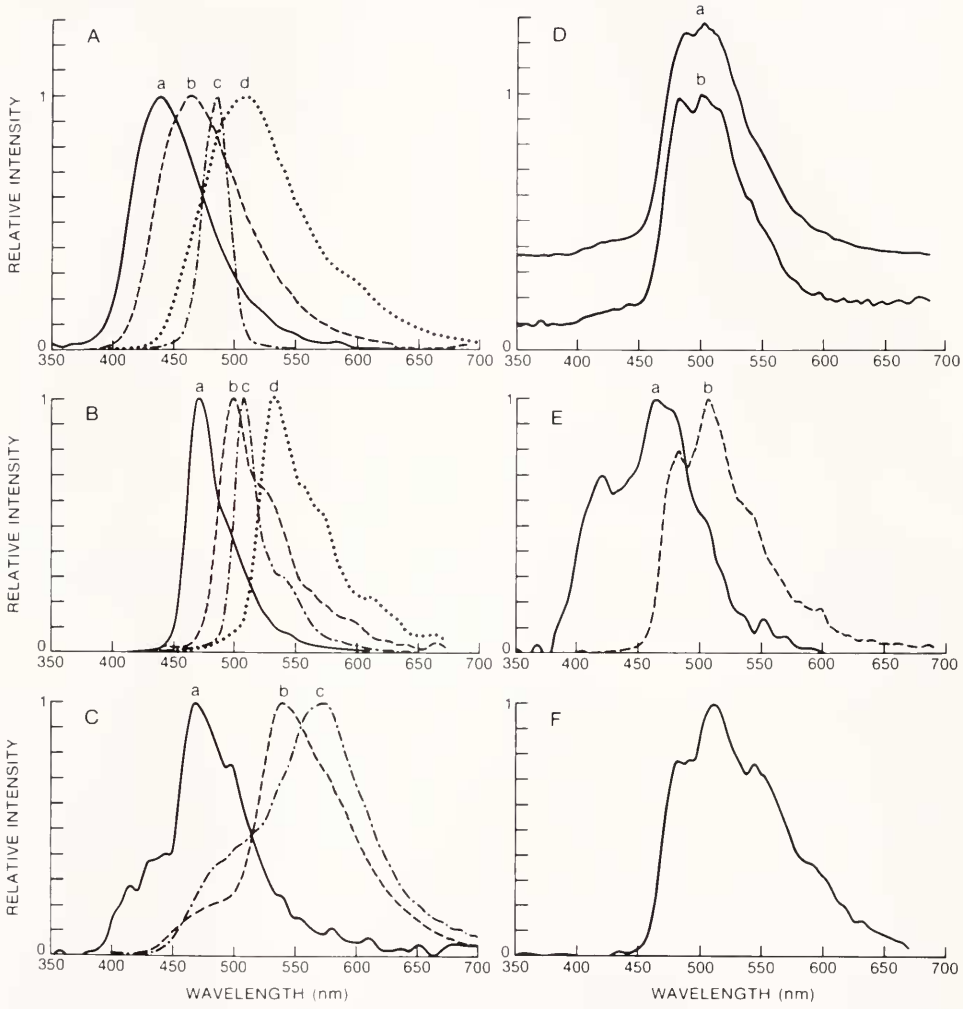

FIGURE 4. Some representative emission spectra of marine organisms. Relative intensity is shown with respect to wavelength. (A) Structureless unimodal distributions. (a) *Scina cf. rattrayi,* λ_{max} = 439 nm, FWHM = 70 nm, S/N = 48; (b) *Vargula hilgendorfii,* λ_{max} = 465 nm, FWHM = 83 nm, S/N = 101; (c) *Argyropelecus affinis,* λ_{max} = 487 nm, FWHM = 26 nm, S/N = 125; (d) *Cleiodopus gloria-maris* adult, λ_{max} = 506 nm, FWHM = 92 nm, S/N = 264. The polychromator spectral window was set for 400–750 nm for (d) and 350–700 nm for (a–c). (B) Unimodal distributions with one or more long wavelength shoulders. (a) *Pyrocystis noctiluca,* λ_{max} = 472 nm, FWHM = 35 nm, S/N = 180; (b) *Pennatula phosphorea,* λ_{max} = 500 nm, FWHM = 53 nm, S/N = 45; (c) *Renilla köllikeri,* λ_{max} = 509 nm, FWHM = 22 nm, S/N = 199; (d) *Stachyptilum superbum,* λ_{max} = 533 nm, FWHM = 58 nm, S/N = 78. (C) Unimodal distributions with short wavelength shoulder. (a) *Sergestes similis,* λ_{max} = 469 nm, FWHM = 62 nm, S/N = 18; (b) *Vibrio fischeri* Y-1 strain at 20°C, λ_{max} = 540 nm, FWHM = 81 nm, S/N = 333; (c) *Parazoanthus lucificum,* λ_{max} = 574 nm, FWHM = 94 nm, S/N = 56. The bumps in (a) are due to random fluctuations (noise) which are present in all spectra but are only apparent at low signal to noise ratios. (D) Bimodal emission spectra of *Porichthys notatus.* (a) Spectrum from ventral photophores viewed by double lens optics, λ_{max} = 488, 504 nm, FWHM = 76 nm, S/N = 130; (b) spectrum from single photophore measured with fiber optic, λ_{max} = 484, 501 nm, FWHM = 75 nm, S/N = 64. The curves are standardized to the same scale but are vertically displaced. (E) Emission spectra of squids displaying a short wavelength secondary peak and long wavelength shoulders. (a) *Abraliopsis falco,* λ_{max} = 421, 466 nm, FWHM = 105 nm, S/N = 12; (b) *Cranchia scabra,* λ_{max} = 483, 511 nm, FWHM = 77 nm, S/N = 63. (F) Trimodal emission spectrum of *Ophiopholis* cf. *longispina,* λ_{max} = 483, 512, 545 nm, FWHM = 102 nm, S/N = 42.

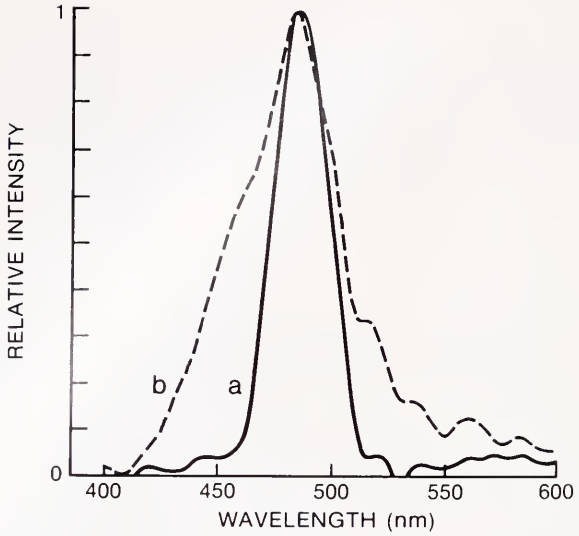

FIGURE 5. Effect of filters in the photophores of a single specimen of *Argyropelecus affinis* on emission spectra. Measured with fiber collection optics; relative intensity displayed as function of wavelength. (a) Emission of posterior photophores, λ_{max} = 486 nm, FWHM = 29 nm, S/N = 15; (b) spectral emission of anterior photophores with ventral tip excised, λ_{max} = 484 nm, FWHM = 53 nm, S/N = 9.

lens collection optics appeared to be bimodal (Fig. 6A). Examination with the fiber bundle collection optics showed that some polyps produced different unimodal emission spectra (Fig. 6B) with a difference in emission maxima of 70 nm. Due to its dimness, this spectral shift was much more difficult to distinguish visually than the 30 nm difference displayed by different *Stachyptilum* colonies. A different colony of the same *Parazoanthus* species had only one emission spectrum which matched the shorter wavelength spectrum of the two color colony.

In the pinecone fish *Cleidopus gloria-maris* there is a visible color difference between the bacterial light organ of juveniles as compared to adults. Comparison of the emission spectra confirmed a 15 nm short wavelength shift in the adults. The fiber bundle collection optics demonstrated the presence of a pronounced emission gradient across the juvenile light organ that was essentially absent in the adult (Table II). Light from the anterior region of the juvenile light organ had a λ_{max} of 555 nm compared to a λ_{max} of 523 nm measured from the mid region and 516 nm in the posterior region. In the adult, measurements from equivalent regions across a single organ were 506 nm, 506 nm, and 503 nm from anterior to posterior. These emission spectra of both juvenile and adult are very different from the spectrum measured from *Vibrio fischeri* (λ_{max} 492 nm, Table II), the bacterium isolated from light organs of this species (Fitzgerald, 1977).

A similar color gradient was seen in the sea pen *Umbellula* (Table II). Luminescence at the base of the stalk was bright green (λ_{max} = 500 nm) with the narrow bandwidth and long wavelength shoulder typical of *in vivo* pennatulid emissions (Morin and Hastings, 1971b; Wampler *et al.*,1973). Proceeding up the stalk the emission became broader, bluer, and dimmer until at the top of the stalk it had a broad, structureless spectrum with a λ_{max} of 470 nm.

The Y-1 strain of *Vibrio fischeri* is also capable of more than one emission color (Ruby and Nealson, 1977). At 20°C or below, emission is unimodal with a short wavelength shoulder and a λ_{max} of 540 nm. However, upon heating the emission

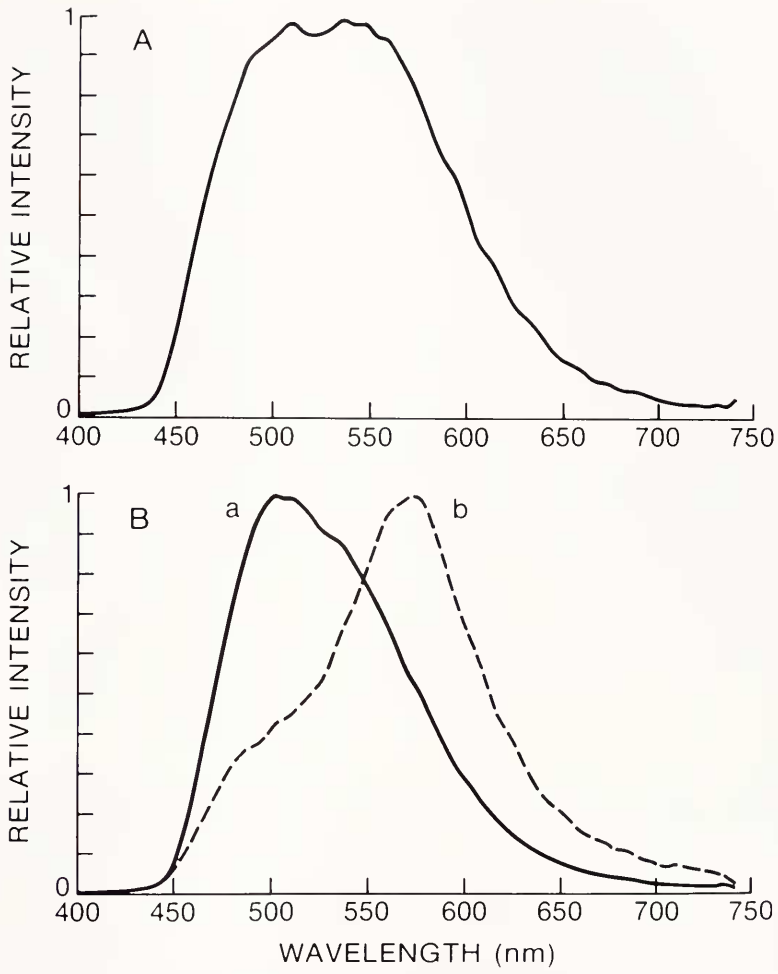

FIGURE 6. Emission spectra of a colony of *Parazoanthus lucificum*. Relative intensity is shown with respect to wavelength. (A) Apparent bimodal spectral distribution from entire colony, measured with double lens collection optics, λ_{max} = 509, 537 nm, FWHM = 140 nm, S/N = 96. (B) Emissions from individuals of colony measured with fiber collection optics. In this colony, two different unimodal distributions were produced, (a) λ_{max} = 502 nm, FWHM = 108 nm, S/N = 145; (b) λ_{max} = 574 nm, FWHM = 94 nm, S/N = 56.

gradually shifts until at 28°C and above the emission is structureless with a λ_{max} of 495 nm.

DISCUSSION

The number of published bioluminescence emission spectra is a small percentage of the total number of luminescent marine species known to exist and the number of accurately determined spectra is probably even smaller. This is largely due to the difficulty of measuring bioluminescence by conventional spectrophotometric techniques. The fragility of marine luminescent organisms demands that the instrumentation be brought to them and the nature of the instrumentation thus far in common use makes this difficult.

The earliest practical spectrophotometric systems used in bioluminescence work were designed for high sensitivity at the expense of resolution. Nicol (*e.g.,* 1958, 1960), using paired photomultipliers, one to correct for total energy variation and the other measuring spectral regions through a series of colored filters, was able to measure dim, relatively long time-course sources such as myctophid photophores, but resolution was limited to approximately 25 nm. Morin and Hastings (1971a, b) utilized a grating monochromator with calibrated photomultiplier to give a calculated bandwidth of 6.6 nm with 4 mm slits. Using a similar system with 2 mm slits, Swift *et al.* (1977) were able to resolve emission peaks 3.5 nm apart. Even though scanning time across the spectrum with the latter system was as short as 3.1 s (Biggley *et al.,* 1981), there was variability in consecutive measurements due to modulations in emission intensity. Other high resolution systems currently in use include Reynolds' (1978) photographic spectroscope-intensifier system and Wampler's spectrofluorometer on-line computer system (Wampler and DeSa, 1971).* The Reynolds system allows simultaneous registration of a wide spectral range (400–600 nm) but in its present configuration it is not amenable to ship-board use and data reduction is time-consuming. The spectrofluorometer system of Wampler utilizes computer software to facilitate data collection, storage, and analysis, but requires scan times of 8 s or longer (Wampler *et al.,* 1971, 1973). For this reason, techniques such as quick freezing and subsequent thawing have been employed to generate steady bioluminescence over the scanning period.

The OMA system, as we have employed it, has three properties essential for determining the emission spectra of living specimens: high sensitivity, high resolution, and simultaneous light collection. It, therefore, represents a practical solution to many problems which have plagued bioluminescence emission spectroscopy, especially with regards to extreme temporal variations of the emissions. For example, luminescent flashes with very fast kinetics such as those produced by myctophid caudal organs (as contrasted with photophores) were easily measured with the OMA in the present study. No published spectra exist for these bright luminescent organs, presumably because irregular flashes of such short duration (60–80 ms, Barnes and Case, 1974) have been impossible to measure with a scanning spectrophotometer.

This system also has the advantage of being able to measure spectra from very localized sources owing to the collection optics employed. The fiber collection optics provide a spatial resolution that has not been previously available. The combination of high sensitivity and spatial resolution allowed convenient measurement of the spectrum of a single photophore (Fig. 4D) and makes the system ideally suited for studying organisms capable of multichromatic emissions. The bichromatic *Parazoanthus lucificum* colony is a dramatic example of the need for this kind of resolving power. Bioluminescence from the colony produced a bimodal spectrum that localized measurements from single polyps resolved into two unimodal peaks. The highest degree of spacial resolution was attained with the pinecone fish, *Cleidopus gloriamaris,* where a gradient of emission was clearly resolved in a light organ measuring only 4 × 2 mm (Haneda, 1966).

In some organisms the chemistry of the luminescent system is responsible for the different colors of emissions. For example, in *Umbellula* the difference in emission between the base and the top of the stalk may be accounted for by different ratios of the two emitters responsible for pennatulid bioluminescence (Wampler *et al.,* 1971, 1973). The emission patterns present in *Umbellula* could involve an increasing con-

* Note: Herring (in press) describes results obtained with a paired scanning photomultiplier system (Collier *et al.,* 1979). This device has a scan time of 30s and a stated accuracy of ±4 nm.

centration of the green fluorescent protein emitter from stalk tip to base that gradually masks the dim blue luciferin emission. The 533 nm emission spectrum from some colonies of the pennatulid *Stachyptilum* is not readily explainable on the basis of the known luciferin and green fluorescent protein emitters responsible for pennatulid luminescence. This emission could be due to a different, undescribed emitter.

Optical filtering may also alter the color of some emissions. In *Argyropelecus* filters narrow the bandwidth of the bioluminescence emission. This may facilitate counterillumination since the maximum and bandwidth of the filtered emission are very similar to that measured for oceanic downwelling irradiance (Young *et al.,* 1980). Filtering may also be responsible for the color of the bacterial light organ of the pinecone fish, *Cleidopus gloria-maris.* The use of filters in the light organ accounts for the difference between the blue-green emission from the intact light organ and the blue luminescence of the bacterial isolates from such organs (Haneda, 1966). The presence of a gradient of emission across the juvenile light organ that is absent in the adults also seems to be due to optical filtering.

The primary value of accumulating a large library of corrected spectra is to classify emitter types. Evidence exists that similar spectra may be due to a common emitter (Wampler *et al.,* 1973). It remains to be seen what chemical relationships exist between organisms that share a common spectral fine structure but emit at different wavelengths, such as the pennatulids already discussed (Fig. 4B) or the squids of Figure 4E. It is also possible that similar spectra in unrelated species may reveal dietary dependencies, although so far where such dependencies have been demonstrated the spectra of predator and prey have been markedly dissimilar (Tsuji *et al.,* 1975; Frank, Widder, Latz and Case, in press).

ACKNOWLEDGMENTS

The authors are indebted to Mark Lowenstine who assisted with installation of the OMA, provided advice on data processing, and has since maintained the system in working order. We also thank Dr. Jeremy Lerner of Instruments SA for suggesting the design of the collection optics. For assistance with animal collection we thank Dr. Peter Anderson, Shane Anderson, Dr. Alissa Arp, Dr. James Childress, John Favuzzi, Tamara Frank, Bill Lowell, and the captains and crews of the "R/V VELERO IV" and "R/V NEW HORIZON." Dr. B. M. Sweeney provided unialgal cultures of all the dinoflagellates and the bacterial isolates of *Abyssicola macrochir* and *Coelorhynchus japonicus;* Dr. Kenneth Nealson generously allowed us to work in his laboratory and provided the remainder of the bacterial cultures. We are grateful to him and to Sea World, San Diego, for providing specimens of *Anomalops* and *Cleidopus* from their displays and to Scripps Aquarium for providing the *Parazoanthus* colonies. Specimens of *Oikopleura* were kindly provided by Dr. Charles Galt. Specimens were identified with the assistance of Dr. F. G. Hochberg, Jr. and Paul Scott of the Santa Barbara Museum of Natural History, Dr. Lawrence Madin of Woods Hole Oceanographic Institution, Dr. Robert Carney of Moss Landing Marine Laboratory, and Dr. Andrew Lisner. This work was supported by a grant from the Office of Naval Research (ONR contract number N00014-75-C-0242), the FBN fund, and faculty research funds from the University of California, Santa Barbara. Work at sea was supported by a grant from the National Science Foundation (OCE 81-10154) to J. J. Childress.

LITERATURE CITED

BARNES, A. T., AND J. F. CASE. 1974. The luminescence of lanternfish (Myctophidae): Spontaneous activity and responses to mechanical, electrical, and chemical stimulation. *J. Exp. Mar. Biol. Ecol.* **15**: 203–221.

BIGGLEY, W. H., T. A. NAPORA, AND E. SWIFT. 1981. The color of bioluminescent secretions from decapod prawns in the genera *Oplophorus* and *Systellaspis* (Caridea). Pp. 66–71 in *Bioluminescence Current Perspectives,* K. H. Nealson, ed. Burgess Publishing Co., Minneapolis.

COLLIER, A. F., R. J. P. BURNHAM, AND P. J. HERRING. 1979. A system for the collection of comparative emission spectra suitable for shipboard use. *J. Mar. Biol. Assoc. U.K.* **59:** 489–495.

DENTON, E. J., J. B. GILPIN-BROWN, AND P. G. WRIGHT. 1970. On the "filters" in the photophores of mesopelagic fish and on a fish emitting red light and especially sensitive to red light. *J. Physiol.* **208:** 72P–73P.

EDWARDS, T. H., AND P. D. WILLSON. 1974. Digital least squares smoothing of spectra. *Appl. Spectrosc.* **28:** 541–545.

FELKEL, H. L., JR., AND H. L. PARDUE. 1979. Simultaneous multielement determinations by atomic absorption and atomic emission with a computerized echelle spectrometer/imaging detector system. Pp. 59–96 in *Multichannel Image Detectors,* Y. Talmi, ed. *Am. Chem. Soc. Symp. Ser.* Washington, DC.

FITZGERALD, J. M. 1977. Classification of luminescent bacteria from the light organ of the Australian pinecone fish, *Cleidopus gloria-maris. Arch. Microbiol.* **112:** 153–156.

FRANK, T. M., E. A. WIDDER, M. I. LATZ, AND J. F. CASE. Dietary maintenance of bioluminescence in a deep-sea mysid. *J. Exp. Biol.* (in press).

HANEDA, Y. 1966. On a luminous organ of the Australian pine-cone fish, *Cleidopus gloria-maris* De Vis. Pp. 547–555 in *Bioluminescence in Progress,* F. H. Johnson and Y. Haneda, eds. Princeton University Press, Princeton.

HERRING, P. J. The spectral characteristics of luminous marine organisms. *Proc. R. Soc. Lond. B.* (in press).

MORIN, J. G., AND J. W. HASTINGS. 1971a. Biochemistry of the bioluminescence of colonial hydroids and other coelenterates. *J. Cell Physiol.* **77:** 305–311.

MORIN, J. G., AND J. W. HASTINGS. 1971b. Energy transfer in a bioluminescent system. *J. Cell. Physiol.* **77:** 313–318.

NICOL, J. A. C. 1958. Observations on luminescence in pelagic animals. *J. Mar. Biol. Assoc. U. K.* **37:** 705–752.

NICOL, J. A. C. 1960. Spectral composition of the light of the lantern fish *Myctophum punctatum. J. Mar. Biol. Assoc. U. K.* **39:** 27–32.

REYNOLDS, G. T. 1978. Application of photosensitive devices to bioluminescence studies. *Photochem. Photobiol.* **27:** 405–421.

RUBY, E. G., AND K. H. NEALSON. 1977. A luminous bacterium that emits yellow light. *Science* **196:** 432–434.

SAVITZKY, A., AND M. J. E. GOLAY. 1964. Smoothing and differentiation of data by simplified least squares procedures. *Anal. Chem.* **36:** 1627–1639.

SELIGER, H. H., J. B. BUCK, W. G. FASTIE, AND W. D. MCELROY. 1964. The spectral distribution of firefly light. *J. Gen. Physiol.* **48:** 95–104.

SWIFT, E., W. H. BIGGLEY, AND T. A. NAPORA. 1977. The bioluminescence emission spectra of *Pyrosoma atlanticum, P. spinosum* (Tunicata), *Euphausia tenera* (Crustacea) and *Gonostoma* sp. (Pisces). *J. Mar. Biol. Assoc. U. K.* **57:** 817–823.

TALMI, Y. 1982. Spectrophotometry and spectrofluorometry with the self-scanned photodiode array. *Appl. Spectrosc.* **36:** 1–18.

TALMI, Y., AND R. W. SIMPSON. 1980. Self-scanned photodiode array: a multichannel spectrometric detector. *Appl. Opt.* **19:** 1401–1414.

TSUJI, F. I., B. G. NAFPAKTITIS, T. GOTO, M. J. CORMIER, J. E. WAMPLER, AND J. M. ANDERSON. 1975. Spectral characteristics of the bioluminescence induced in the marine fish, *Porichthys notatus,* by *Cypridina* (Ostracod) luciferin. *Mol. Cell. Biochem.* **9:** 3–8.

WAMPLER, J. E. 1978. Measurements and physical characteristics of luminescence. Pp. 1–48 in *Bioluminescence in Action,* P. J. Herring, ed. Academic Press, London.

WAMPLER, J. E., AND R. DESA. 1971. An on-line spectrofluorimeter system for rapid collection of absolute luminescence spectra. *Appl. Spectros.* **25**(6): 623–627.

WAMPLER, J. E., K. HORI, J. W. LEE, AND M. J. CORMIER. 1971. Structured bioluminescence. Two emitters during both the *in vitro* and the *in vivo* bioluminescence of the sea pansy, *Renilla. Biochemistry* **10:** 2903–2909.

WAMPLER, J. E., Y. D. KARKHANIS, J. G. MORIN, AND M. J. CORMIER. 1973. Similarities in the bioluminescence from the Pennatulacea. *Biochim. Biophys. Acta* **314:** 104–109.

YOUNG, R. E., E. M. KAMPA, S. D. MAYNARD, F. M. MENCHER, AND C. F. E. ROPER. 1980. Counter-illumination and the upper depth limits of midwater animals. *Deep-Sea Res.* **27A:** 671–691.